VOLUME 112, NUMBER 10
MAY 9, 1990

JOURNAL OF THE AMERICAN CHEMICAL SOCIETY

Conformational Analysis of the Mushroom Toxin Phallacidin by ^1H NMR Spectroscopy and Restrained Molecular Dynamics

P. Bönzli and J. T. Gerig*

Contribution from the Department of Chemistry, University of California, Santa Barbara, California 93106. *Received August 31, 1989*

Abstract: A conformational study of the toxin phallacidin [cyclo(Val[1]-*erythro*-3-hydroxy-D-Asp[2]-Cys[3]-*cis*-4-hydroxy-Pro[4]-Ala[5]-2-mercapto-Trp[6]-4,5-dihydroxy-Leu[7])cyclic(3 → 6) sulfide] has been carried out using PMR spectroscopy and molecular dynamics simulations. An assignment of most of the resonances of the heptapeptide has been achieved, and internuclear distance information has been obtained from rotating frame NOE experiments. Temperature dependences of the amide NH chemical shifts and amide hydrogen–deuterium exchange rates were also examined. Energy minimization and molecular dynamics studies, carried out with the available experimental information as constraints, define the orientations of those parts of the heptapeptide identified as being essential for toxicity and suggest that these groups can maintain their relative orientations in spite of high flexibility in some parts of the peptide backbone.

The bicyclic heptapeptide phallacidin, cyclo(Val[1]-*erythro*-3-hydroxy-D-Asp[2]-Cys[3]-*cis*-4-hydroxy-Pro[4]-Ala[5]-2-mercapto-Trp[6]-4,5-dihydroxy-Leu[7])cyclic(3 → 6) sulfide (**1**), is a representative of the phallotoxins, a family of toxins elaborated by the highly poisonous mushroom *Amanita phalloides*.[1,2] Phallotoxins bind strongly to F-actin and stabilize it against depolymerization by potassium iodide, alkali, DNAse I, heat, or sonication.[3,4] Structural studies have shown that the functional groups of **1** essential for toxicity are the methyl group of Ala[5], the *cis*-hydroxy group of OH-Pro[4], the hydrogen of the indole nitrogen of Trp[6], and the sulfur bridge of Cys[3]; the molecule must be bicyclic to keep these groups in the proper orientation for binding.

Knowledge of molecular conformation is indispensable in attempts to understand biological activity. However, little is known about the three-dimensional structure of the phallotoxins since attempts to determine their structure by X-ray diffraction have been frustrated by the inability to crystallize them. A study of phalloidin, another phallotoxin, has been carried out by NMR spectroscopy and conformational energy calculations,[5] but these results were obtained before the advent of modern NMR techniques and are somewhat ambiguous.

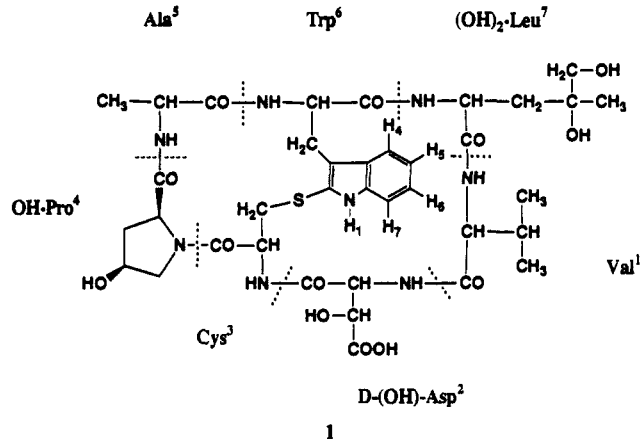

1

The development of two-dimensional NMR spectroscopy has provided efficacious methods for conformational analysis of cyclic

* To whom correspondence should be addressed.

(1) Wieland, T. *Science* **1968**, *159*, 946–952.
(2) Wieland, T. *CRC Crit. Rev. Biochem.* **1978**, *5*, 185–260.
(3) Wieland, T. *Adv. Enzyme Regulation* **1977**, *15*, 285–300.

0002-7863/90/1512-3719$02.50/0

peptides of 4–10 amino acids.[6] We have applied these methods, other PMR observations, and restrained molecular dynamics calculations in an attempt to define the conformation of **1** in DMSO-d_6 solution. Although meeting suggested criteria for conformational homogeneity,[7] the structure refined by molecular dynamics simulations using proton–proton distances from ROESY experiments as constraints showed a backbone conformation with higher flexibility than might be expected from the NMR results. Independent flips of the peptide units between [OH-Pro^4, Ala^5] and between [Trp^6, (OH)$_2$-Leu^7] were observed in these simulations, but generally these only affected ψ_i, and ϕ_{i+1} at each residue, leaving ω_i unchanged and producing only minor perturbations of the overall topology of the backbone. Similar events in other cyclic peptides of this size have been reported to occur in solution[6i,8] and in the solid state.[9]

Experimental Section

Phallacidin (**1**) was purchased from Sigma (90% purity). A 8.4 mM solution was prepared by dissolving 5 mg in 0.7 mL of DMSO-d_6 (Aldrich, 99.9% D, degassed) and placed in a 5-mm tube. All operations were carried out in a glovebox under a nitrogen atmosphere to minimize the presence of adventitious water.

Proton NMR spectra were recorded at 500 MHz with use of a General Electric GN-500 spectrometer. Chemical shifts are reported relative to the signal of DMSO-d_6, which was assigned 2.49 ppm. Sample temperatures were controlled with the variable temperature unit of the instrument and are believed to be accurate to ±2 °C. The 90° proton pulse was 9–10 μs and was checked frequently.

Double quantum-filtered phase-sensitive COSY spectra[10a,b] were recorded at 60 °C by using the pulse sequence 90–t_1–90–δ–90–acquisition with phase sensitivity achieved by using the TPPI method.[10c] Sixteen scans were recorded into 4K data blocks for each of 449 t_1 values with a relaxation delay of 3 s, the time δ, to permit rf phase shifting, set to 3 μs, and spectral widths in f_1 and f_2 of 7042 Hz. The data matrix was zero-filled to 4 K in f_1, apodized with a double exponential function, and symmetrized after transformation. Data were plotted in the absolute value mode.

NOESY spectra were recorded at 23 °C under similar conditions with a mixing time of 300 ms.[11]

One-dimensional NOE difference spectra were recorded at 75 °C according to the procedure of Sanders et al.[12]

ROESY spectra were recorded at 75 °C with the pulse sequence 90_x–t_1–$(\beta_y$–$\tau)_n$–acquisition.[13] For the spin-locking field the repetitive pulse sequence $(\beta$–$\tau)_n$ was used with a flip angle $\beta = 32°$ as it has been suggested that a small flip angle in this sequence leads to suppression of cross peaks due to coherence transfers between scalar-coupled spins (*J* peaks),[13] although this result has been questioned.[14] In a typical experiment spectra were collected into 2K data blocks for 690 t_1 increments with a relaxation delay of 3 s, $\tau = 3$ μs, $n = 5000$–9500 to give a mixing time of 180–330 ms with a locking field of 2.22 kHz. Spectral widths in both dimensions were 6200 Hz. Phase sensitivity was achieved by the States method.[15] The data matrix was zero filled to 2K in f_1 and apodized with exponential functions to give line broadening of 0.5 Hz in f_2 and 5 Hz in f_1. Data were analyzed both with and without symmetrization.

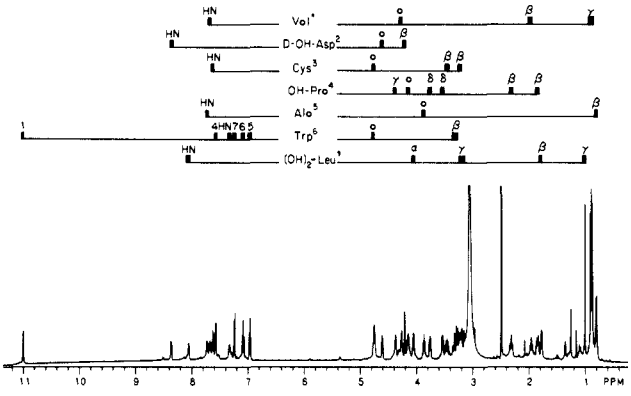

Figure 1. One-dimensional 500 MHz ^{1}H NMR spectrum of phallacidin in DMSO-d_6 solution at 85 °C with the assignment of the proton chemical shifts as discussed in the text.

ROESY experiments with mixing times of 180, 220, and 330 ms were performed in order to check linearity of the ROE buildup. ROESY cross peaks are dependent on offset from the rf carrier.[6g,16] With medium-sized molecules which give no appreciable NOE in the laboratory frame and the assumption that all proton–proton interactions can be described by the same correlation time, the offset dependence can be corrected by using the following formula,[6g] where I_{ab} is the cross peak intensity, r_{ab} the distance between protons a and b, B_1 the field strength of the locking field, and ω_i the resonance offset of nucleus i.

$$r^6_{ab} = K \sin^2(\beta_a) \sin^2(\beta_b)/I_{ab}$$

$$\beta_i = \arctan(\gamma B_1/\omega_i)$$

The constant K can be evaluated from the cross peaks developed between protons of known separation. Distances between the geminal protons at OH-ProH$^\beta$,OH-ProH$^\beta$ (1.78 Å) and the HN–H$_7$ distance in the indole ring of Trp^6 (2.82 Å[17]) were used as standards for this determination. The K values obtained with the different calibration distances were in good agreement for mixing times of 220 and 180 ms, but at 330 ms the data were more scattered, suggesting that spin diffusion is beginning to occur at this mixing time. Agreement of the K values for different calibration distances suggests that coherence transfers between adjacent protons (e.g., the geminal protons of the pyrrolidine ring) are not significant contributors to the ROESY cross peaks analyzed, although the similar frequency offsets of some pairs of protons would favor such transfers. The values in Table IV are the averages of distances obtained at 180 and 220 ms.

Hydrogen–deuterium exchange of acidic protons was followed at 45 °C. The exchange was initiated by adding sufficient D_2O (99.8%, Aldrich) to the peptide sample in DMSO-d_6 to give a 10% solution. Spectra were recorded at various times between 7 and 1300 min after addition of the D_2O and worked up under standard conditions. The extent of exchange was estimated from peak areas or integrals.

Molecular dynamics calculations were performed on a Silicon Graphics 4D/70 computer by using the program CHARMM (Version 21).[18] The molecular graphics program QUANTA (Polygen, Version 2.0) was used for generation and analysis of structures and for plotting. The empirical energy function includes harmonic potential energy terms for bond lengths, bond angles, dihedral angles, improper dihedral angles, and

(4) Miyamoto, Y.; Kuroda, M.; Munekata, E.; Masaki, T. *J. Biochem.* **1986**, *100*, 1677–1680.
(5) Patel, D. J.; Tonelli, A. E.; Pfaender, P.; Faulstich, H.; Wieland, T. *J. Mol. Biol.* **1973**, *79*, 185–196.
(6) For recent examples, see: (a) Kessler, H.; Kogler, H. *Liebigs Ann. Chem.* **1983**, 316–329. (b) Pelton, J. T.; Whalon, M.; Cody, W. L.; Hruby, V. J. *Int. J. Peptide Protein Res.* **1988**, *31*, 109–115. (c) Kessler, H.; Bermel, W.; Müller, A.; Pook, K.-H. In *The Peptides: Analysis, Synthesis, Biology*; Udenfried, S., Meienhofer, J., Hruby, V. J., Eds.; 1985; Vol. 7, pp 437–473. (d) Bruch, M. D.; Noggle, J. H.; Gierasch, L. M. *J. Am. Chem. Soc.* **1985**, *107*, 1400–1407. (e) Baniak, E. L.; Rivier, J. E.; Struthers, R. S.; Hagler, A. T.; Gierasch, L. M. *Biochemistry* **1987**, *26*, 2642–2652. (f) Giralt, E.; Felitz, M. *Magn. Reson. Chem.* **1985**, *24*, 123–129. (g) Kessler, H.; Bats, J. W.; Griesinger, C.; Koll, S.; Will, M.; Wagner, K. *J. Am. Chem. Soc.* **1988**, *110*, 1033–1049. (h) Kessler, H.; Klein, M.; Wagner, K. *Int. J. Peptide Protein Res.* **1988** *31*, 481–498. (i) Hruby, V. J.; Kao, L.-F.; Pettitt, B. M.; Karplus, M. *J. Am. Chem. Soc.* **1988**, *110*, 3351–3359. (j) Lautz, J.; Kessler, H.; Boelens, R.; Kaptein, R.; van Gunsteren, W. F. *Int. J. Peptide Protein Res.* **1987**, *30*, 404–414.
(7) Kessler, H. *Angew. Chem., Int. Ed. Engl.* **1982**, *21*, 512–523.
(8) Kessler, H.; Griesinger, C.; Lautz, J.; Müller, A.; van Gunsteren, W. F.; Berendsen, H. J. C. *J. Am. Chem. Soc.* **1988**, *110*, 3393–3396.
(9) Kople, K. D.; Bhandary, K. K.; Kartha, G.; Wang, Y.-S.; Parameswaran, K. N. *J. Am. Chem. Soc.* **1986**, *108*, 4637–4642.
(10) (a) Piantini, U.; Sørensen, O. W.; Ernst, R. R. *J. Am. Chem. Soc.* **1982**, *104*, 6800–6901. (b) Rance, M.; Sørenson, O. W.; Bodenhausen, G.; Wagner, G.; Ernst, R. R.; Wüthrich, K. *Biochem. Biophys. Res. Commun.* **1983**, *117*, 479–485. (c) Marion, D.; Wüthrich, K. *Biochem. Biophys. Res. Commun.* **1983**, *113*, 976–974.
(11) Kumar, A.; Wagner, G.; Ernst, R. R.; Wüthrich, K. *J. Am. Chem. Soc.* **1981**, *103*, 3654–3658.
(12) Sanders, J. K. M.; Mersh, J. D. *Prog. NMR Spectrosc.* **1982**, *15*, 353–400.
(13) Kessler, H.; Griesinger, C.; Kerssebaum, R.; Wagner, K.; Ernst, R. R. *J. Am. Chem. Soc.* **1987**, *109*, 607–609.
(14) Bax, A. *J. Magn. Reson.* **1988**, *77*, 134–142.
(15) States, D. J.; Haberkorn, R. A.; Ruben, D. J. *J. Magn. Reson.* **1982**, *48*, 286–292.
(16) Griesinger, C.; Ernst, R. R. *J. Magn. Reson.* **1987**, *75*, 261–271.
(17) Bye, E.; Mostad, A.; Rømming, C. *Acta Chem. Scand.* **1973**, *27*, 471–484.
(18) Brooks, B. R.; Bruccoleri, R. E.; Olafson, B. D.; States, D. J.; Swaminathan, S.; Karplus, M. *J. Comput. Chem.* **1983**, *4*, 187–217.

Table I. Proton Chemical Shifts of Phallacidin[a]

proton	Val	D-OH-Asp	Cys	OH-Pro	Ala	Trp[b]	$(OH)_2$-Leu[c]
NH	7.68	8.35	7.62		7.73	7.33	8.06
H^{α}	4.26	4.59	4.75	4.15	3.86	4.75	4.05
$H^{\beta pro\text{-}S}$	1.96		3.20[d]	1.85	0.81	3.27	1.76
$H^{\beta pro\text{-}R}$		4.20	3.46[d]	2.31		3.34	1.76
$H^{\gamma pro\text{-}S}$	0.90						
$H^{\gamma pro\text{-}R}$	0.88			4.37			
$H^{\delta pro\text{-}S}$				3.54			3.14[d]
$H^{\delta pro\text{-}R}$				3.76			3.20[d]

[a] In ppm, measured at 500 MHz with a DMSO-d_6 solution at 85 °C. [b] Chemical shifts of the indole protons: NH, 11.00; H_4, 7.57; H_5, 6.96; H_6 7.08; H_7 7.24. [c] CH_3 shift, 1.00. [d] Stereospecific assignment is ambiguous.

functions for van der Waals, electrostatic, nonbonding and hydrogen-bonding interactions. Solvent molecules were not explicitly included in our calculation, but their effects were simulated by using a distance-dependent dielectric constant, $\epsilon = R_{ij}$.[17,19] Distance constraints were implemented by adding extra harmonic terms of the form $E = K(R - R_o)^2$, with $K = (SkT\delta_l^{-2})/2$ for $R < R_o$ and $K = (SkT\delta_h^{-2})/2$, for $R > R_o$ to the energy function,[20] where δ_l and δ_h are the low and high distance error estimates, k is the Boltzmann constant, T is the temperature, and S is a constant. At $\delta_l = \delta_h = 0.2$ Å K was set to equal 149 kcal mol^{-1} Å^{-2}, while at $\delta_l = \delta_h = 0.4$ Å K was set to equal 37 kcal mol^{-1} Å^{-2}, with $T = 300$ K and $S = 1$. Of the 29 proton–proton distances determined by the ROESY experiments, the 16 indicated in Table VII were directly relevant to the conformation of the peptide backbone. These were included as constraints in the dynamics simulation with error limits set between 0.2 and 0.4 Å, the error limit used being roughly proportional to the reliability with which the corresponding cross peak intensity could be determined in the ROESY experiments.

Structures were minimized by using the adopted basis Newton–Raphson algorithm (ABNR). Carbon–hydrogen bond lengths were kept constant by using the SHAKE method, with a relative tolerance of 10^{-10}.[21] Nonbonded interactions were switched off by using a cubic switching function between 10.5 and 11.5 Å with pairs of atoms up to 12 Å included in the nonbonded list. Initial step sizes for the minimization algorithm were set to 0.02 Å. Calculations were run until the change in computed energy between iterations was less than 0.1 cal/mol. By using this convergence criterion minimizations usually converged within 200 steps.

Dynamic calculations were performed by use of the Verlet algorithm.[22] During the heating and equilibration periods the velocities of the atoms were reassigned to the appropriate temperature (300 K) every 0.2 ps, while the list of nonbonded and hydrogen bonded interactions was updated every 10 fs. The time step for the integration was 1 fs.

Results and Discussion

Chemical Shift Assignment and Coupling Constants. A prerequisite for elucidation of the solution conformation of a peptide is unambiguous assignment of the PMR chemical shifts and coupling constants. Our assignment of the spectrum of **1** is summarized in Table I and Figure 1 and is based mainly on the connectivity information via scalar coupling in double quantum-filtered COSY experiments. The spin systems of Val[1], D-OH-Asp[2], OH-Pro[4], and Ala[5] were readily identified by their characteristic spin-coupling patterns, and, in these cases, all resonances could be assigned. For OH-Pro[4] the diastereotopic protons H^{β} and H^{δ} could be identified by using coupling information and H–H distances from ROESY spectra, as indicated below.

The $(OH)_2$-Leu$^7H^{\delta}$ protons were hidden under the water resonance at 60 °C. They were identified at 85 °C by a decoupling experiment, but a stereospecific assignment was not possible. The broad, temperature-dependent line widths observed for the $(OH)_2$-Leu$^7H^{\beta}$ resonances suggests flexibility within this residue, with these signals being near the intermediate exchange regime.

Trp$^6H^{\alpha}$ and Cys$^3H^{\alpha}$ peaks strongly overlap at temperatures between 25 °C and 85 °C so that the AMXY spin systems of these two amino acids could not be distinguished. The NH protons could be assigned by their ROESY cross peaks to H^{α} protons at neighboring amino acids, and the H^{β} protons then be identified by computer simulations of the two-spin systems. With the assigned couplings $J(C^{\alpha},NH)$, the two possible splittings of the strongly overlapping H^{α} resonances were simulated by interchanging the two sets of $H^{\alpha},H^{\beta pro\text{-}R}/H^{\alpha},H^{\beta pro\text{-}S}$ couplings. Only one solution was in agreement with the experimental spectrum. The tentative stereospecific assignment of the diastereotopic β protons of Trp^6 is based on the large trans coupling of $H^{\beta pro\text{-}S}$ to H^{α} (J = 11.6 Hz). This assignment was in agreement with the ROESY data. Assignment of the Cys$^3H^{\beta}$ resonances remains ambiguous due to the lack of reliable distance information.

Vicinal proton coupling constants show a Karplus-type dihedral angular dependence and thereby provide conformational information.[23,24] For example, $J(NH,H^{\alpha})$, dependent on the torsion angle ϕ, yields information about the backbone conformation, while H^{α},H^{β} coupling constants similarly can define side-chain conformations. Various coupling constants for **1** were extracted from a 1D spectrum at 85 °C (Figure 1) and are given in Table II.

Table II. Vicinal ^1H, ^1H Coupling Constants of Phallacidin

J (Hz)	Val	D-OH-Asp	Cys	OH-Pro	Ala	Trp	$(OH)_2$-Leu
NH,H^{α}	6.8	7.8	7.2		6.4	9.3	5.0
$H^{\alpha},H^{\beta pro\text{-}S}$	6.8		9.0[a]	8.6	7.5	11.6	
$H^{\alpha},H^{\beta pro\text{-}R}$		4.8	4.2[a]	4.2		5.2	
$H^{\beta pro\text{-}R},H^{\beta pro\text{-}S}$			13.0	14.1		15.6	
$H^{\beta pro\text{-}S},H^{\gamma}$	6.8			5.4			
$H^{\beta pro\text{-}R},H^{\gamma}$				4.9			
$H^{\gamma},H^{\delta pro\text{-}S}$				4.1			
$H^{\gamma},H^{\delta pro\text{-}R}$				5.1			
$H^{\delta pro\text{-}R},H^{\delta pro\text{-}S}$				10.3			

[a] Stereospecific assignment is ambiguous.

Table III. J (NH,H^{α}) Coupling Constants and Corresponding Dihedral Angles[a]

	J (NH,H^{α}), Hz	θ, deg	ϕ, deg
Val	6.8	25, 140	35, 85, −160, −80
D-OH-Asp	7.8	20, 145	−40, −80, 85, 155
Cys	7.2	20, 140	40, 80, −160, −80
Ala	6.4	30, 140	30, 90, −160, −80
Trp	9.3	0, 155	60, −145, −95
$(OH)_2$-Leu	5.0	40, 125	100, 20, −65, −175

[a] θ and ϕ, derived from the Karplus-type equation of Bystrov[23] as described in the text. θ is the angle between the projection of the bonds N–H and C^{α}–H^{α} on a plane perpendicular to the N–C^{α} axis and is related to the dihedral angle ϕ by $\theta = |60° - \phi|$.

Scalar couplings of the hydroxyproline[4] ring were obtained by first-order analysis. The assignment of the shifts and couplings of the diastereotopic H^{β} and H^{δ} protons was based on the H,H distances to H^{α} and H^{δ} indicated by ROESY experiments. Identification using J values alone is ambiguous in some cases as, for example, the value for $J(H^{\alpha},H^{\beta pro\text{-}S})$ (8.6 Hz) could correspond to either a cis or trans interaction. From the set of coupling constants obtained the conformation of the pyrrolidine ring could be deduced and is defined by $\chi^1 \cong 10°$ and $\chi^2 \cong -45°$.

One H^{α},H^{β} coupling of Cys^3 was not accessible due to strong overlap of H^{β} with $(OH)_2$-Leu^7-H^{δ}. However, the value of this coupling constant could approximately be determined by computer simulation of the splitting pattern of the overlapping H^{α} protons of Cys^3 and Trp^6. This procedure did not permit stereospecific assignment, and the ROESY cross peaks to H^{α} which potentially could have resolved the problem by providing distance information

(19) Gelin, B. R.; Karplus, M. *Proc. Natl. Acad. Sci. U.S.A.* **1975**, *72*, 2002–2006.
(20) (a) Kaptein, R.; Zuiderberg, E. R. P.; Scheek, R. M.; Bolens, R.; van Gunsteren, W. F. *J. Mol. Biol.* **1985**, *182*, 179–182. (b) Brünger, A. T.; Clore, G. M.; Gronenborn, A. M.; Karplus, M. *Proc. Natl. Acad. Sci. U.S.A.* **1986**, *83*, 3801–3805.
(21) van Gunsteren, W. F.; Berendsen, H. J. C. *Mol. Phys.* **1977**, *34*, 1311–1327.
(22) Verlet, L. *Phys. Rev.* **1967**, *159*, 98–103.
(23) Bystrov, V. F. *Prog. NMR Spectrosc.* **1976**, *10*, 41–82.
(24) Bystrov, V. F.; Arseniev, A. S.; Gavrilov, Y. D. *J. Magn. Reson.* **1978**, *30*, 151–184.

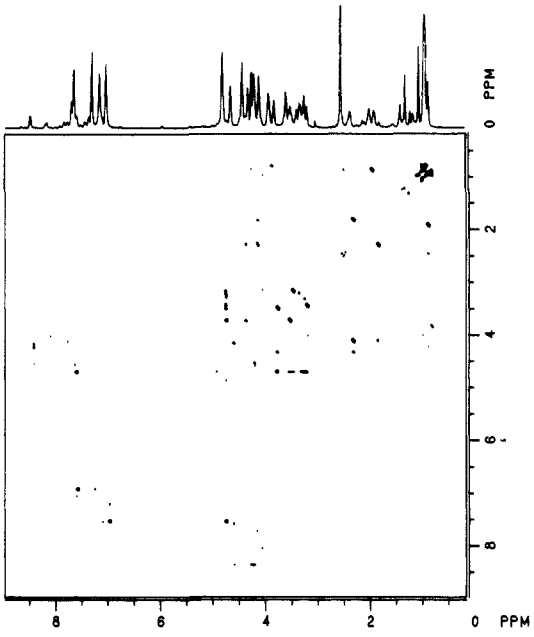

Figure 2. Plot of a portion of a 500 MHz ROESY spectrum of phallacidin in DMSO-d_6 solution at 75 °C. A mixing time of 220 ms was used; only negative peaks due to cross-relaxation in the rotating frame are shown.

were obscured by t_1-noise. The diastereotopic H^β protons of Trp[6] were distinguished by the large trans coupling between H^α and $H^{\beta_{pro\text{-}S}}$.

The broad resonances of the H^β protons of $(OH)_2$-Leu[7] afforded little information about the side-chain conformation of this residue.

The amide doublets of Val[1], Ala[5], Trp[6], and $(OH)_2$-Leu[7] were not completely resolved under these conditions, and the apparent values for $J(NH,H^\alpha)$ were therefore corrected by using the method of Bystrov.[23] The coupling constants obtained strongly resemble those reported for phalloidin.[5] Table III summarizes $J(NH,H^\alpha)$ values obtained and indicates possible values for ϕ derived from the Karplus-type equation given by Bystrov.

Proton–Proton Distances. At 500 MHz and room temperature **1** exhibits only weak, negative nuclear Overhauser effects in 1D NOE difference experiments, and two-dimensional NOESY spectra contained only a few weak cross peaks. It is apparent that the correlation time for this medium-sized molecule is such that the cross relaxation rate $(W_2 - W_0)$ is near zero. In this situation the determination of H,H distances by 2D rotating frame cross relaxation experiments is expected to yield better results.[25,26] ROESY data were collected with various mixing times; the results shown in Figure 2 are typical of those obtained. Table IV records average values for 29 proton–proton distances in **1** obtained by ROESY experiments by using three calibration distances and 180 and 220 ms mixing time data.

Temperature Dependence; H,D Exchange Rates. Most of the chemical shifts of **1** are slightly temperature dependent over the range 25 °C to 85 °C with both upfield and downfield shifts with increasing temperature observed. The largest temperature dependences were exhibited by the Ala[5] methyl (about 2 ppb/°C upfield), the β-proton of Val[1] (about 1.2 ppb/°C downfield), and the α-proton of Asp[2] (about 1.8 ppb/°C downfield). In no case was there a significant change in the nature of the spin-coupling multiplet, suggesting that large changes in conformation do not take place over this temperature range. Spectral lines were somewhat sharper at the higher temperatures, and these were preferred for most of the experiments carried out.

Information about the chemical environment of the amide protons of phallicidin can be obtained from the temperature dependence of the chemical shifts. Changes of the NH resonances

Table IV. Proton–Proton Distances (Å) in Phallacidin[a]

$ValH^\alpha$,AspNH	2.5	$ProH^{\beta_{pro\text{-}R}}$,$ProH^\gamma$	2.3
$ValH^\alpha$,$ValH^\beta$	2.4	$ProH^{\beta_{pro\text{-}S}}$,$ProH^\gamma$	2.4
$ValH^\beta$,$ValH^\gamma$	2.1	$ProH^\gamma$,$ProH^{\delta_{pro\text{-}R}}$	2.3
AspNH,$AspH^\alpha$	2.9	$ProH^\gamma$,$ProH^{\delta_{pro\text{-}S}}$	2.7
AspNH,$AspH^\beta$	2.6	$ProH^\alpha$,AlaNH	2.9
AspNH,CysNH	3.5	$AlaH^\alpha$,AlaNH	2.9
$AspH^\alpha$,CysNH	2.6	$AlaH^\alpha$,$AlaH^\beta$	2.1
$AspH^\alpha$,$AspH^\beta$	2.4	TrpNH,$TrpH^\alpha$	3.4
CysNH,$CysH^\alpha$	2.9	$TrpH^\alpha$,$TrpH_4$	2.3
$CysH^\alpha$,$CysH^{\beta_{pro\text{-}R}}$	2.4[b]	$TrpH_7$,$TrpH_6$	2.1
$CysH^\alpha$,$ProH^{\delta_{pro\text{-}R}}$	2.2	$TrpH_4$,$TrpH_5$	2.2
$CysH^\alpha$,$ProH^{\delta_{pro\text{-}S}}$	2.4	$LeuH^\alpha$,LeuNH	2.8
$CysH^{\beta_{pro\text{-}R}}$,$CysH^{\beta_{pro\text{-}S}}$	2.2	$LeuH^\alpha$,$LeuH^\beta$	2.2
$ProH^\alpha$,$ProH^{\beta_{pro\text{-}R}}$	2.3	$LeuH^\alpha$,Leu(CH_2-O)	2.3
$ProH^\alpha$,$ProH^{\beta_{pro\text{-}S}}$	2.4		

[a] Obtained from ROESY experiments at 500 MHz, sample DMSO-d_6 at 75 °C. For the following interactions no distances could be obtained due to t_1 noise: $CysH^\alpha$,$CysH^{\beta_{pro\text{-}S}}$; $TrpH^\alpha$,$TrpH^{\beta_{pro\text{-}R}}$; $TrpH^\alpha$,-$TrpH^{\beta_{pro\text{-}S}}$; $ValH^\alpha$,$ValH^\gamma$; $TrpH^\alpha$,LeuNH. The cross peak for $TrpH_5$,$TrpH_6$ was too close to the diagonal to be used reliably. No cross peak for the $ValH^\alpha$,ValNH interaction was observed. [b] Only one of two possible cross peaks was observed between $CysH^\alpha$ and $CysH^\beta$. Stereospecific assignment of this cross peak was not possible, and indication of the β-proton is arbitrary.

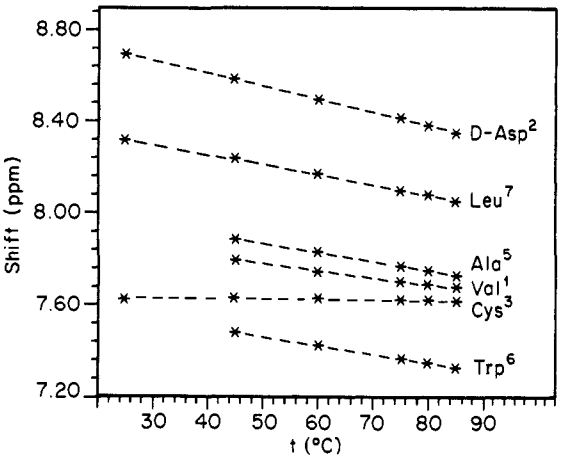

Figure 3. Plot of the temperature dependence of the amide proton chemical shifts of phallacidin between 25 °C and 85 °C. The shifts are relative to DMSO-d_6. The slopes $(-\Delta\delta/\Delta T)$ in ppb/°C are as follows: Val^1 2.8; D-$OH\text{-}Asp^2$ 5.7; Cys^3 0.3; Ala^5 4.0; Trp^6 3.6; $(OH)_2$-Leu^7 4.3.

with temperature are related to their ability to participate in intermolecular hydrogen bonds.[27,28] Generally temperature gradients exceeding 4 ppb/°C are considered to be evidence for an external NH orientation, while values smaller than 2 ppb/°C are indicative intramolecular hydrogen bonding.[29] Temperature dependences of the amide proton chemical shifts of **1** are illustrated in Figure 3. The amide NH of Cys^3 is relatively unaffected by changing temperature and is, therefore, likely involved in intramolecular hydrogen bonding. ROESY data and the probable value of ϕ for D-$OH\text{-}Asp^2$ (85 °C) suggest that the NH of Cys^3 is hydrogen bonded to CO of Val^4 as part of a γ-turn.[30] All other NH proton shifts exhibit slopes consistent with a more external orientation. The linearity of the temperature dependences for all the N–H shifts is a strong indication that major conformational changes are absent in the temperature range 25 °C to 85 °C.[6c]

Exchange rates of the amide protons were studied by adding 10% D_2O to a sample of **1** in DMSO-d_6 at 45 °C. The amide protons of D-$OH\text{-}Asp^2$, Ala^5, and indole NH of Trp^6 exchange

(25) Bothner-By, A. A.; Stephens, R. L.; Lee, J.; Warren, C. D.; Jeanloz, R. W. *J. Am. Chem. Soc.* **1984**, *106*, 811–813.
(26) Bax, A.; Davis, D. G. *J. Magn. Reson.* **1985**, *63*, 207–213.
(27) Urry, D. W.; Ohnishi, M.; Walter, R. *Proc. Natl. Acad. Sci. U.S.A.* **1970**, *66*, 111–116.
(28) Torchia, D. A.; Wong, S. C. K.; Deber, C. M.; Blout, E. R. *J. Am. Chem. Soc.* **1972**, *94*, 616–620.
(29) Bara, Y. A.; Friedrich, A.; Kessler, H.; Molter, M. *Chem. Ber.* **1978**, *111*, 1045–1057.
(30) Rose, G. D.; Gierasch, L. M.; Smith, J. A. *Adv. Protein. Chem.* **1985**, *37*, 1–109.

rapidly, and their signals disappeared within 7 min under these conditions. The Val[1]-NH has a half-life of approximately 7 min and the $(OH)_2$-Leu[7]-NH, about 10 m. Exchange of Cys[3]-NH and Trp[6]-NH was much slower, half-lives of 8 h and >20 h, respectively, being observed for these amide resonances. From these data it was concluded that all amide protons except those of Cys[3] and Trp[6] are oriented away from the core of the peptide and are probably involved in forming intermolecular hydrogen bonds. The result for Cys[3]-NH is in agreement with the implication of the observed weak dependence of its chemical shift on temperature and further supports intramolecular hydrogen bonding of this group. The amide NH of Trp[6] has a large temperature dependence but a very slow exchange rate. There are many cases where the implications of the temperature dependence of a peptide N–H shift are not in agreement with deuterium exchange rate studies,[31] and it may be that the TrpN-H, although internally buried, is only weakly hydrogen bonded, if at all.

Structural Refinement by Restrained Molecular Dynamics (MD). To translate the proton–proton distances and other experimental information into a three-dimensional structure the method of restrained molecular dynamics simulation was used.[6g,j,19,32] In contrast to energy minimization, which only explores the conformation of a single static structure, a MD simulation can overcome energy barriers of the magnitude kT and carry the system into regions of other conformational energy minima, depending on the kinetic energy of the system and the time allowed to search conformational space. The analysis of a dynamics trajectory also provides insight into the flexibility of a molecule.

Computer model building was used to construct a variety of starting conformations for phallacidin, all being in agreement with the constraints imposed by the NMR data. Consonant with most cyclic peptides of similar size, all amide bonds were assumed to be trans. Critical to the conformation is the region of the Cys[3]-OH/Pro[4] amide bond since ROESY cross peaks between Cys[3]H$^{\alpha}$ and OH-Pro[4]H$^{\delta}$ could only be observed if this amide group is in a trans conformation. Moreover, the presence of the Cys[3]-NH-Val[1]-CO hydrogen bond and the ROE distances observed are only compatible with the presence of a γ-turn involving residues Val[1] and Cys[3]. Finally, the number of possible conformations is limited by the presence of the Cys[3]-Trp[6] bridge. Conformations developed by these methods and consistent with the constraints mentioned mainly differed in the ϕ angles of the backbone, especially where the information from H,H coupling constants in this regard is ambiguous. For D-OH-Asp[2], Cys[3], and Trp[6] only one set of ϕ angles was consistent with a reasonable structure for **1**, but for Val[1], Ala[5], and $(OH)_2$-Leu[7] several ϕ angles were compatible with experimental results.

The initial structure derived from model building which best fit the NMR data was subjected to conformational energy minimization with the inclusion of 16 H,H distance constrains derived from the ROESY experiments listed in Table IV. Only structurally significant interproton distances between protons of the backbone including H$^{\beta}$ protons that could be unambiguously assigned, the methylene bridges of Cys[3] and Trp[6], and the indole ring were used, while distances between protons of the highly flexible side chains and the pyrrolidine protons of HO-Pro were omitted.

Subsequently a 54 ps restrained molecular dynamics calculation was performed. In the first 3 ps the initial velocities of the atoms were steadily increased to reach the kinetic energy corresponding to 300 K. In the equilibration phase from 3–4.6 ps the velocities were reassigned to a Maxwellian distribution at 300 K every 0.2 ps in order to remove "hot spots" in the molecule. The time period between 5.4 and 54 ps was used in a "production dynamics" run with velocities, coordinates, and energies saved every 0.1 ps.

Backbone Conformation. Examination of the dynamics trajectory suggests that phallacidin is a relatively flexible molecule.

Table V. Energy Terms for Conformers **1a** to **1e** of Phallacidin (kcal/mol)[a]

energy	1a	1b	1c	1d	1e
torsion	23.47	21.28	16.33	20.56	24.86
van der Waals	−9.10	−8.96	−11.09	−13.03	−12.84
bond angle	11.61	13.07	10.98	9.81	10.98
bond	1.20	1.12	1.10	1.01	0.97
electrostatic	−119.01	−121.50	−122.92	−131.69	−115.88
NOE constraints	2.79	3.24	3.88	6.35	4.73
total	−88.46	−90.36	−99.59	−105.33	−89.23

[a] Minimization was done on each conformation, applying the same distance constraints as for the molecular dynamics simulation.

Table VI. Dihedral Angles of Conformers **1a–e**[a]

		1a	1b	1c	1d	1e	av
Val	ϕ	−77	−73	−72	−61	−75	−68
	ψ	68	91	77	82	78	83
D-OH-Asp	ϕ	80	88	116	76	82	82
	ψ	−49	−51	−75	−70	−56	−63
	χ_1	−176	−176	178	−179	−173	−178
Cys	ϕ	−60	−60	−82	−68	−69	−70
	ψ	142	159	155	134	141	137
	χ_1	31	−62	−14	32	36	17
OH-Pro	ϕ	−69	−79	−75	−53	−56	−63
	ψ	65	48	54	−58	−50	−3
	χ_1	29	35	35	22	23	27
	χ_2	−40	−41	−41	−35	−37	−37
Ala	ϕ	171	177	−175	−62	−67	−112
	ψ	−37	−66	−56	−35	−11	−43
Trp	ϕ	−95	−65	−66	−73	−113	−75
	ψ	175	113	−17	−20	180	−13
	χ_1	−36	−32	−45	−45	−45	−42
$(OH)_2$-Leu	ϕ	−69	−32	78	73	81	71
	ψ	−51	−51	−62	−56	−54	−52
	χ_1	169	177	−173	−177	−172	−177

[a] Conformations **1a–d** are obtained from the average of coordinates from the dynamics trajectory of the following time intervals: **1a**, 8.5–9.0 ps; **1b**, 19.1–20.0 ps; **1c**, 24.1–25.0 ps; **1d**, 37.1–38.0 ps. **1e** was obtained from **1a** by rotating the peptide unit between OH-Pro[4],Ala[5] using the procedure described in the text. The average structure (last column) was obtained by averaging coordinates observed over the entire dynamics simulation (4.6–54 ps). In all cases, the angles ω were close to 180° (trans amide bonds).

Table VII. Comparison of Selected Distances in Conformations of Phallacidin[a]

	Exp	1a	1b	1c	1d	1e
ValH$^{\alpha}$,ValNH	[b]	2.85	2.73	2.75	2.90	2.89
ValH$^{\alpha}$,ValH$^{\beta}$	2.4	2.91	2.94	3.04	2.83	3.00
ValH$^{\alpha}$,AspNH	2.5	2.45	2.72	2.44	2.22	2.52
AspNH,AspH$^{\alpha}$	2.9	2.88	2.96	2.90	2.90	2.92
AspNH,AspH$^{\beta}$	2.6	2.65	2.37	2.49	2.54	2.73
AspNH,CysNH	3.5	3.54	3.39	3.68	3.53	3.54
AspH$^{\alpha}$,CysNH	2.6	2.61	2.93	2.80	2.72	2.67
AspH$^{\alpha}$,AspH$^{\beta}$	2.4	2.42	2.52	2.70	2.65	2.43
CysH$^{\alpha}$,ProH$^{\delta_{pro\text{-}R}}$	2.2	2.30	2.50	2.49	2.34	2.34
CysH$^{\alpha}$,ProH$^{\delta_{pro\text{-}S}}$	2.4	2.34	2.29	2.39	2.20	2.41
CysNH,CysH$^{\alpha}$	2.9	2.83	2.95	2.91	2.89	2.90
ProH$^{\alpha}$,AlaNH	2.9	2.56	2.87	2.69	3.53	3.47
AlaNH,AlaH$^{\alpha}$	2.9	2.78	2.83	2.68	2.92	2.89
TrpNH,TrpH$^{\alpha}$	3.4[c]	2.90	2.95	2.93	2.90	2.98
TrpH$^{\alpha}$,TrpH$_4$	2.3	2.21	2.61	2.35	2.08	2.14
LeuH$^{\alpha}$,LeuNH	2.8	2.90	2.56	2.50	2.20	2.91

[a] Conformations **1a–e** defined as described in Table VI. [b] The ROESY spectra contains no cross peak for this interaction. The largest feasible distance (2.9 Å[38]) was used as a constraint but with a large error limit (0.4 Å). [c] Distances between H$^{\alpha}$ and NH can vary between 2.15 and 2.9 Å.[38] The experimental distance is unreasonable, and a value of 2.9 Å was assumed.

(31) Jardetzky, O.; Roberts, G. C. K. *NMR in Molecular Biology*; Academic: New York, 1981; p 166.

(32) For examples of this procedure, see: (a) Clore, G. M.; Gronenborn, A. M.; Brünger, A. T.; Karplus, M. *J. Mol. Biol.* **1985**, *186*, 435–455. (b) Clore, G. M.; Brünger, A. T.; Karplus, M.; Gronenborn, A. M. *J. Mol. Biol.* **1986**, *191*, 523–551. (c) Kaptein, R.; Zuiderweg, E. R. P.; Schoek, R. M.; Bolens, R.; van Gunsteren, W. R. *J. Mol. Biol.* **1985**, *182*, 179–182. (e) Kaptein, R.; Bolens, R.; Scheek, R. M.; van Gunsteren, W. F. *Biochemistry* **1988**, *27*, 5389–95.

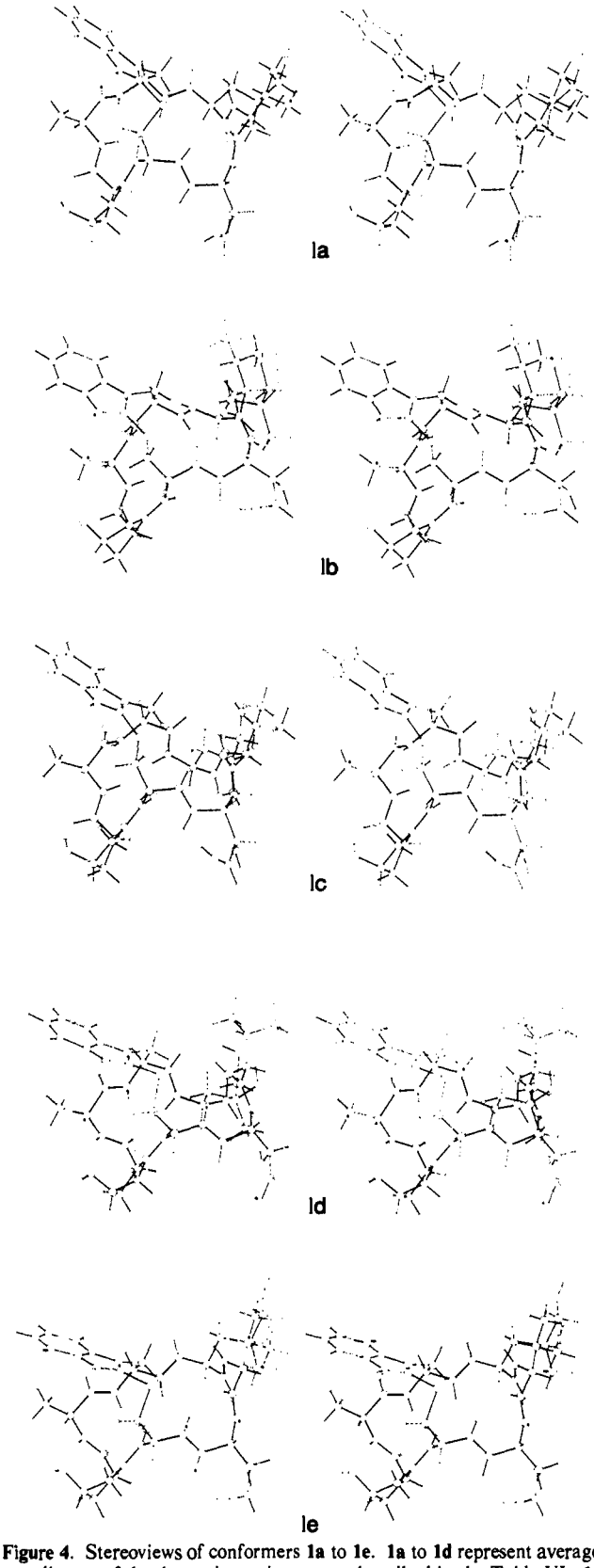

Figure 4. Stereoviews of conformers **1a** to **1e**. **1a** to **1d** represent average coordinates of the dynamics trajectory as described in the Table VI. **1e** was obtained from **1a** by a rotation of ψ from OH-Pro^4 from 78° to −60° as described in the text.

Several significantly different backbone conformers that were observed during the 54 ps dynamics simulation are shown in Figure 4. Conformations **1a–d** were obtained by calculating average coordinates for the time intervals 8.5–9.0 ps (**1a**), 19.1–20.0 ps (**1b**), 24.1–25.0 ps (**1c**), and 37.1–38 ps (**1d**). As discussed below conformation **1e** was generated from **1a** by changing ψ of OH-Pro

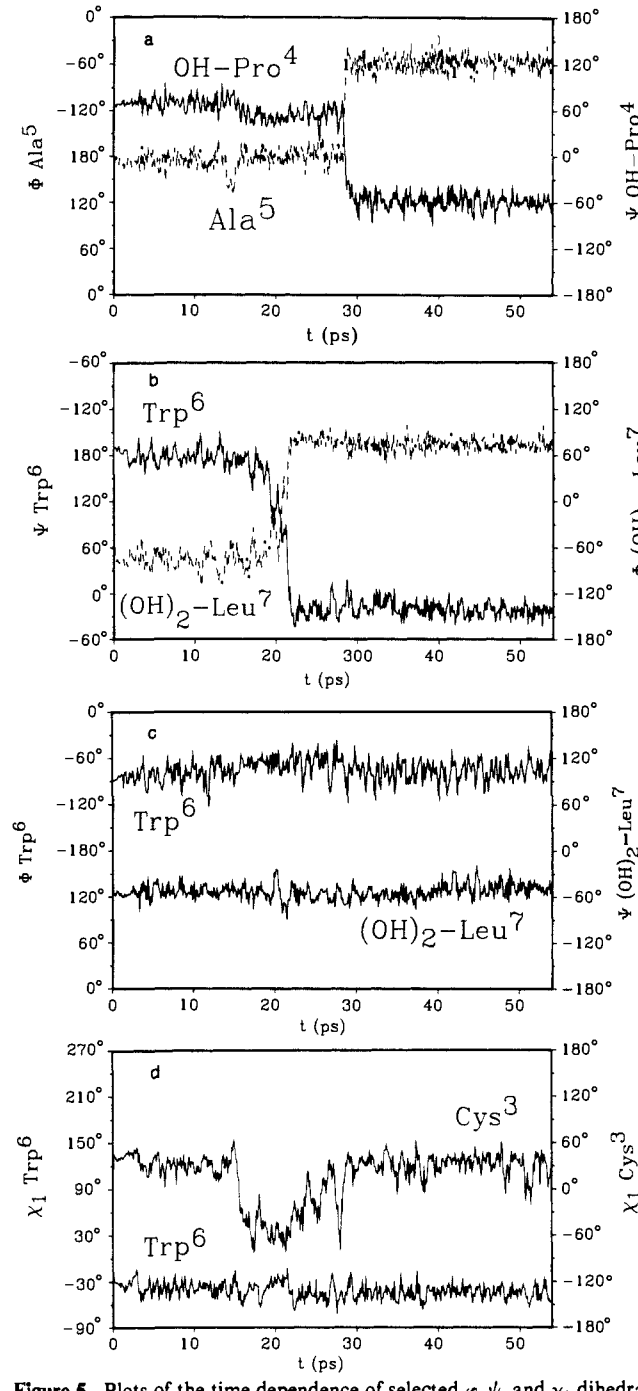

Figure 5. Plots of the time dependence of selected φ, ψ, and χ_1 dihedral angles observed during the molecular dynamics simulation of phallacidin. Panel a shows rotation of the peptide unit between OH-Pro^4 and Ala^5 (**1c** to **1d** transition). Panel b indicates the rotation of the peptide unit between Trp^6 and (OH)$_2$-Leu^7 (**1a** to **1b**).

from 65° to −50°. Structures **1a–e** were each minimized, and the resulting empirical energies of each are listed in Table V, while the bond angles and interproton distances characteristic of these appear in Tables VI and VII.

Between 19 and 21 ps of the simulation the starting conformation **1a** undergoes a flip of the peptide unit between Trp^6 and (OH)$_2$-Leu^7 of about 200° by synchronous changes of the adjacent ϕ and ψ angles giving conformation **1c**. This flip proceeds in two stages through an intermediate state (**1b**) wherein the carbonyl oxygen of Trp^6 is hydrogen bonded with Cys^3-NH ($\psi_6 \cong 110°$). In conformation **1b** the O–H bond length is ca. 2.5 Å, while the average value of this bond length over the entire period of the dynamics simulation was 5.3 Å. A separate, apparently independent 120° flip of the peptide unit between OH–Pro and Ala^6 appears at 28.5 ps, converting conformation **1c** into **1d**. Both of

these flips are evident in plots of the time dependence of internuclear distances or the torsion angles ϕ and ψ (Figure 5). Interestingly, only the adjacent torsions are affected by the flips, while all other dihedrals remain nearly constant during these processes.

Since the peptide flips seem to take place independently, conformation **1e** can also be predicted. This structure was not observed during the course of the dynamics trajectory but is reasonably postulated to form by flip of the peptide unit between the hydroxyproline and alanine residues.

A rough estimate of the free energy barrier for rotation of the peptide unit between HO-Pro^4 and Ala^5 can be obtained by noting that one of these events was observed over the time course of the dynamics simulation. An event every 60 ps corresponds to a barrier of 3.7 kcal/mol. Another approach is to carry out a series of calculations in which ψ of HO-Pro^4 is incremented, with energy minimization being done at each step. By this second procedure the energy barrier to rotation of the peptide unit between HO-Pro^4 and Ala^5 (**1c** to **1d** transition) was estimated to be about 7 kcal mol^{-1}, and the barrier for the transition **1a** to **1c** was computed to be about 18 kcal mol^{-1}. The true rotational barriers are probably overestimated by this second approach because in the simulations only adjacent ϕ and ψ angles were varied, leaving the remaining backbone unaffected. This approach introduces strain energy into the system, especially for the rotation of the amide group between Trp^6 and (OH)$_2$-Leu^7 (**1a** → **1c**), where the temporary formation of a hydrogen bond (conformation **1b**) is involved. Minor changes in other parts of the backbone, not taken into account, would relieve strain and lower the energy barrier to rotation accordingly. Thus, the results of the second estimation procedure are not inconsistent with the first estimate.

These peptide group rotations cause only local changes in the topology of the molecule, and the overall backbone conformation of conformations **1a–e** are very similar. These conformations are computed to be similar in energy, with **1d** favored by these empirical energy calculations. Given the differences in energy predicted for each of the conformations it is possible that phallicidin is able to exist in several distinct relatively long-lived conformations rather than simply undergoing fluctuations about a single conformation. However, the energy differences are mainly due to the electrostatic energy term, and the contribution of this component to the total energy may be overemphasized.

Side-Chain Conformations. The conformational mobilities of the side chains of Cys^3 and Trp^6 are strongly restricted by the bridge between them. The experimental distance between indole H_4 and Trp^{6}H$^\alpha$ (2.3 Å), the large $J(H^\alpha,H^{\beta_{pro-S}})$ coupling constant (11.6 Hz), and the distances between Cys-H$^\alpha$ and HO-Pro-H$^\delta$ (2.2 and 2.4 Å) further reduce the number of conformations possible for this part of the molecule. Within these constraints there is some flexibility available for the S–Cβ bond of Cys^3, where χ_1 can switch between 40° and −60° (Figure 5d). All other torsions were found to be invariant for the time period of the dynamics simulation. Fluctuations about the S–Cβ bond only effect the conformation of the Cys^3 methylene group, leaving the overall topology of the molecule essentially unchanged.

The methyl group of Ala^5 is in a quasi-equatorial position in the conformations we have found and is computed to be, on average, about 5 Å away from the face of the six-membered indole ring. Alanine methyl protons would normally be expected to exhibit a chemical shift of 1.22 ppm.[33] However, the protons of a methyl group oriented in the manner indicated would experience a ring current shift of about 0.4 ppm from the indole ring of the tryptophan residue,[34] giving an expected chemical shift (0.82 ppm) in good agreement with the experimental value (0.81 ppm).

In the MD calculations the conformation of the pyrrolidine ring of HO-Pro^4 (the γ-hydroxy group in a quasi-axial position with C$_\gamma$ in the exo position relative to the HO-Pro^4 carbonyl group) was invariant during the period of the simulation. The torsion angles $\chi^1 = 27°$ and $\chi^2 = -37°$, averaged over the 4.6–54 ps part of the dynamics trajectory, are consistent with observed vicinal coupling constants. There was no indication of an endo/exo equilibrium due to a flip of C$_\gamma$, and, in general, fluctuations of the ring carbons were small.

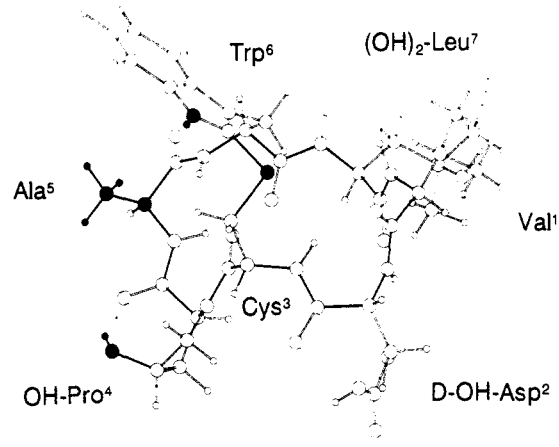

Figure 6. Conformation **1a** of phallacidin with the functional groups essential for toxicity shown in black.

The side-chain conformation of D-HO-Asp^2 seems to be largely determined by a hydrogen bond formed between the carboxylic proton with D-HO-Asp^2 CO.

There is little information about the local conformations of the side chains of Val^1 and (OH)$_2$-Leu^7 from our NMR data. While the presence of staggered rotamers of (OH)$_2$-Leu^7 with $\chi^1 = 60°$, −60°, and 180° is presumably possible, it was unfeasible to estimate the relative population of these, for example, by application of Pachler's equations,[35] because the chemical shifts of the H$_\beta$ protons were nearly coalesced between 25 °C and 85 °C so that $J_{\alpha,\beta}$ for their coupling could not be determined. The coalescence of these shifts, however, is an indication of rotation of this residue either around the C$_\alpha$–C$_\beta$ or C$_\beta$–C$_\gamma$ bond. The MD simulations indicate that rotations of these side chains are slow relative to the time scale of the MD simulation done. As the side chains of Val^1 and (OH)$_2$-Leu^7 do not appear to be relevant for the biological activity of phallicidin, a lack of conformational information about them does not severely reduce the utility of the conformational analysis.

Figure 6 depicts phallacidin in conformation **1a** with the parts of the structure that are essential for biological activity highlighted. There were no major changes in the relative orientations of these groups, despite the flexibility of the peptide backbone of **1**, during the course of the dynamics simulation. While it is possible that the conformation of phallacidin is substantially altered when the polypeptide binds to actin, such alterations would come at an appreciable energy cost in terms of the development of unfavorable interactions within the peptide. It is suggested that the conformation(s) of **1** detected in our work provide at least a reasonable starting point for defining features of the three-dimensional structure of the actin receptor site for this peptide.

Derivatives of the phallotoxins have been successfully used to characterize the state of f-actin in cells.[36,37] Whether or not side-chain derivatization alters the conformation of **1** and the interaction with f-actin are presently under investigation.

Summary. Combined use of PMR experiments and restrained molecular dynamics simulations provide sufficient information to define many aspects of the solution conformation of phallicidin. This peptide appears not to exist solely in a single conformation

(33) Wüthrich, K. *NMR in Biological Research: Peptides and Proteins*; North-Holland, Amsterdam, 1976; p 51.
(34) Johnson, C. E.; Bovey, F. A. *J. Chem. Phys.* **1958**, *29*, 1012–1014.
(35) (a) Pachler, K. G. R. *Spectrochim. Acta* **1963**, *19*, 2085–2092. (b) Pachler, K. G. R. *Spectrochim. Acta* **1964**, *20*, 581–587.
(36) Faulstich, H.; Zobeley, S.; Rinnerthaler, G.; Small, J. V. *J. Muscle Res. Cell. Motility* **1988**, *9*, 370–383.
(37) Faulstich, H.; Zobeley, S.; Bentrup, U.; Jockusch, B. M. *J. Histochem. Cytochem.* **1989**, *37*, 1035–1045.
(38) Wüthrich, K. *NMR of Proteins and Nucleic Acids*; Wiley: New York, 1986; p 119.

but, because of flexibility in the backbone of the molecule, likely equilibrates through at least four distinguishable conformations. Empirical energy calculations indicate that electrostatic interactions are a major determinant of conformation in this molecule. MD simulations constrained by NOE distance information suggest that functional groups essential for biological activity maintain essentially the same relative orientations over the time course of the calculations. Although the reasons for the extremely tight binding of phallicidin to actin are not revealed by our conformational studies of the peptide, there is nothing apparent in these results to indicate what would be gained by a significant conformational deformation of phallicidin upon binding to actin. Our results may, therefore, prove useful in mapping the features of the actin-binding site that are complimentary to the structure of this peptide.

Acknowledgment. This work was supported by the California Cancer Research Coordinating Committee and, in part, by NIH Grant GM25975. We are indebted to Professor T. C. Bruice for access to his Silicon Graphics system and to D. H. Gregory for his assistance with some of the calculations.

Registry No. Phallacidin, 26645-35-2.

Multiple-Quantum NMR in a Mixture of Liquid Crystals: Differential Coherence Development†

W. V. Gerasimowicz,*,‡ A. N. Garroway, and J. B. Miller

Contribution from the Chemistry Division, Code 6122, Naval Research Laboratory, Washington, D.C. 20375-5000. *Received October 31, 1989*

Abstract: A 2:1 molar mixture of 4′-(cyanophenyl)-4-*n*-heptylbenzoate and 4′-(cyanophenyl)-4-*n*-butylbenzoate exhibits nematic liquid crystal behavior in the temperature range from 25 °C to 50 °C. The proton NMR spectra suggest that two regimes of dipolar interaction are present, i.e., those characteristic of nearly isolated proton spin pairs, presumably on the phenyl rings, and weakly coupled multispin clusters originating from the alkyl chain moieties comprising the remainder of the system. A solid-echo pulse sequence permits the observation and separation of these unique regions within the molecules on the basis of their differing relaxation properties. We have combined this solid echo selection technique with multiple-quantum NMR. Differential development of proton spin coherence can then be distinguished (in this case) for *different* segments of the *same* molecule. We find that over the course of the multiple-quantum preparation times, the phenyl proton spin pairs do not interact appreciably with the remaining protons of the molecule.

Introduction

Time-resolved multiple-quantum nuclear magnetic resonance spectrometry (MQ NMR) has been demonstrated to be an effective means for determining the spatial distribution of nuclei in materials which lack long-range order. Much of the work has been performed in the liquid state where the size of spin systems which have been investigated is relatively small.[1-11] The operator formalism for double quantum NMR transitions of dipolar-coupled spin pairs (prior to the advent of time-reversal pulse sequences) has been discussed.[12] The introduction of time-reversal pulse sequences has made the investigation of larger spin systems, including those in solids, feasible.[13-15] Proton MQ NMR has been applied to NMR and imaging in solids,[16-19] the study of hydrogen distribution in solids,[14,19] and in the determination of hexamethylbenzene distribution in Na-Y zeolite samples.[20]

Nematic liquid crystals have also been the subject of a number of MQ NMR investigations.[11,15,21,22] In the case of nematic liquid crystal samples, intermolecular proton dipolar couplings are averaged to zero, while intramolecular couplings remain significant.[23] The elimination of intermolecular dipolar coupling is attributed to the rapid translational diffusion which nematic liquid crystalline molecules undergo. Such liquid crystal samples have been treated as idealized cases of isolated spin clusters on the NMR time scale, i.e., the individual molecules behave as if they are solid clusters which are independent of one another.[11,15,21,22] Furthermore, the development of multiple-quantum coherence within such systems (or the correlation of the ^1H spins within the molecule) has been analyzed on the basis that the pattern and rate of growth of such correlations reflects the distribution of atoms within the system.

In this article we present an example of a mixture of 4′-(cya-

* Author to whom correspondence should be addressed.

† Presented in part at the 29th Experimental Nuclear Magnetic Resonance Spectroscopy Conference, Rochester, NY, April 1988.

‡ Permanent address: United States Department of Agriculture, Agricultural Research Service, North Atlantic Area, Eastern Regional Research Center, 600 E. Mermaid Lane, Philadelphia, PA 19118.

(1) Bodenhausen, G. *Prog. NMR Spectrosc.* **1981**, *14*, 137.
(2) Piantini, U.; Sorenson, O. W.; Ernst, R. R. *J. Am. Chem. Soc.* **1982**, *104*, 6800.
(3) Bax, A.; Freeman, R.; Kempsell, S. P. *J. Am. Chem. Soc.* **1980**, *102*, 4849.
(4) Bax, A.; Freeman, R.; Kempsell, S. P. *J. Magn. Reson.* **1980**, *41*, 349.
(5) Bax, A.; Freeman, R.; Frenkiel, T. A. *J. Am. Chem. Soc.* **1981**, *103*, 2102.
(6) Bax, A.; Freeman, R.; Frenkiel, T. A.; Levitt, M. H. *J. Magn. Reson.* **1981**, *43*, 478.
(7) Braunschweiler, L.; Bodenhausen, G.; Ernst, R. R. *Mol. Phys.* **1983**, *48*, 535.
(8) Levitt, M. H.; Ernst, R. R. *Chem. Phys. Lett.* **1983**, *100*, 119.
(9) Warren, W. S.; Weitekamp, D. P.; Pines, A. *J. Chem. Phys.* **1980**, *73*, 2084.
(10) Warren, W. S.; Pines, A. *J. Chem. Phys.* **1981**, *74*, 2808.
(11) Sinton, S.; Zax, D. B.; Murdoch, J. B.; Pines, A. *Mol. Phys.* **1984**, *53*, 333.
(12) Vega, S.; Pines, A. *J. Chem. Phys.* **1977**, *66*, 5624.
(13) Yen, Y. S.; Pines, A. *J. Chem. Phys.* **1983**, *78*, 3579.
(14) Baum, J.; Munowitz, M.; Garroway, A. N.; Pines, A. *J. Chem. Phys.* **1985**, *83*, 2015.
(15) Shykind, D. N.; Baum, J.; Liu, S.-B.; Pines, A.; Garroway, A. N. *J. Magn. Reson.* **1988**, *76*, 149.
(16) Drobny, G.; Pines, A.; Sinton, S.; Weitekamp, D. P.; Wemmer, D. *Faraday Symp. Chem. Soc.* **1979**, *13*, 49.
(17) Bodenhausen, G.; Vold, R. L.; Vold, R. R. *J. Magn. Reson.* **1980**, *37*, 93.
(18) Pines, A. In *Proceedings of the Fermi School on the Physics of NMR in Biology and Medicine*; Maraviglia, B., Ed.; In press.
(19) Garroway, A. N.; Baum, J.; Munowitz, M. A.; Pines, A. *J. Magn. Reson.* **1984**, *60*, 337.
(20) Ryoo, R.; Liu, S.-B.; de Menorval, L. C.; Takegashi, K.; Chmelka, B.; Trecoske, M.; Pines, A. *J. Phys. Chem.* **1987**, *91*, 6575.
(21) Sinton, S.; Pines, A. *Chem. Phys. Lett.* **1980**, *76*, 263.
(22) Munowitz, M.; Pines, A. *Science* **1986**, *233*, 525.
(23) De Gennes, P. G. *The Physics of Liquid Crystals*; Clarendon Press: Oxford, 1974.